Effect of unsteady uniform inflow on the stability of tidal turbine wake vortices

Amanda S. M. Smyth, Takafumi Nishino, and Anna M. Young

Abstract—**We report on the observation of vortex instabilities in the wake of a tidal turbine undergoing axially oscillating inflow, using unsteady RANS simulations. Unsteady inflow causes the turbine blades to shed vorticity of time-varying strength into the wake, which in turn leads to a spatial variation in wake vortex strength, such that the vorticity of adjacent returning wake segments can differ. This spatial variation triggers the instability of tip vortices, the characteristics of which are shown to be governed by the 'frequency ratio' $\omega/\Omega N_B$ (where ω is harmonic inflow frequency, Ω is turbine rotational frequency and N_B is the number of blades). If $\omega/\Omega N_B = m$, where m is an integer, the wake is stable. If $\omega/\Omega N_B$ takes the form of $1/m$ or $(m-1)/m$, however, m adjacent tip vortices start leapflogging and merging into a larger vortex, creating a new vortex street with a lower spatial frequency. At other frequency ratios, the tip vortices exhibit more irregular deformation, suggesting a possible early breakdown into turbulence. This has implications for both wind and tidal farm design, where the interaction of downstream turbines with the wakes of upstream turbines is an important consideration.**

Index Terms—**Tidal turbine, Wake development, Vortex instability, Unsteady flow.**

I. Introduction

HELICAL vortices shed from rotating blades are of concern in many engineering applications. In wind and tidal power generation, these vortices may affect the performance of not only the turbine shedding them (via the interaction of 'returning wake' and the blades; see, e.g. [1], [2]) but also other turbines located downstream, as the stability of these vortices dictates the length of 'near-wake' region and thus the onset of 'far-wake' recovery process [3].

The existence of 'mutual-inductance' instability was first reported by Widnall [4], who conducted a linear stability analysis of a single helical vortex filament to calculate the growth rate of small sinusoidal perturbations of various wavelengths. Since then many theoretical [5]–[7], experimental [8]–[10] and numerical [11]–[13] studies have been reported on how the instability leads to pairing/leapfrogging and eventual breakdown of helical vortices shed from a rotor. Based on a linear stability analysis with numerical observations of tip-vortex breakdown using large-eddy simulations (LES), Sørensen et al. [14] proposed a semi-analytical model of turbine near-wake length as a function of the turbine thrust, tip-speed ratio and inflow turbulence intensity. Such a vortex breakdown model may be adopted to improve low-order models of wind and tidal turbine wakes, such as those based on Reynolds-averaged Navier-Stokes (RANS) actuator disc approaches (with a special treatment of the near-wake region to make its length adjustable; see [15]) and more computationally inexpensive 'engineering' wake models [16].

Since an early breakdown of tip vortices may help reduce the wake length and thus improve the power of downstream turbines, it is of great interest to find a practical method to enhance the breakdown. Some recent numerical studies suggest that, for wind turbines, it is possible to accelerate the near-wake breakdown by perturbing tip vortices via the actuation of trailing-edge flaps employed in the outboard region of blades [17] or even via the control of blade pitch and rotor speed [18], especially when the inflow turbulence level is low. For tidal turbines, however, it is still unclear how beneficial such an active control could be as they usually operate in a highly turbulent flow. Moreover, tidal turbines are often subject to an oscillatory inflow due to surface waves, which may cause strong periodic perturbations of the helical wake vortices.

In this paper we present some preliminary results of wake instability in a model tidal turbine subjected to harmonic axial inflow conditions in unsteady RANS simulations. The purpose is to observe how these harmonic inflow perturbation affect the stability and development of the turbine wake.

II. Methodology

A. Mathematical model

We solve the 3-D incompressible unsteady RANS equations numerically, using the open source CFD software OpenFOAM [19], to simulate the flow past a tidal turbine rotor. The Reynolds stresses are computed using the shear-stress transport (SST) k-omega model [20].

It should be noted that the unsteady RANS simulations performed in this study are unable to capture the exact process of tip-vortex breakdown. Using a standard or 'fully turbulent' RANS model (such as the SST k-omega model adopted here) to simulate helical wake vortices behind a rotor is somewhat analogous to using a fully turbulent model to simulate a transitional boundary layer on an aerofoil. The results are inevitably inaccurate as the turbulent kinetic energy (and thus the eddy viscosity) is incorrectly produced

A. S. M. Smyth and T. Nishino are departmental lecturers at the Department of Engineering Science, University of Oxford, Parks Road, Oxford OX1 3PJ, U.K. (e-mail: amanda.smyth@eng.ox.ac.uk and takafumi.nishino@eng.ox.ac.uk).

A. M. Young is a senior lecturer at the Department of Mechanical Engineering, University of Bath, Claverton Down, Bath BA2 7AY, U.K. (e-mail: amy32@bath.ac.uk).

Digital Object Identifier:
https://doi.org/10.36688/ewtec-2023-454

by a (practically) non-turbulent shear layer forming a vortex. However, these simulations are still useful for studying the flow physics before the onset of the breakdown process (where the viscosity has only a secondary effect on the dynamics of vortices) as well as after the breakdown process (where the flow is fully turbulent). It should also be noted that, even with 'eddy-resolved' simulations such as LES, the exact process of vortex breakdown may or may not be captured depending on the resolution used.

B. Vortex dynamics

Numerical studies of helical wake vortex breakdown have traditionally only considered the tip vortices, neglecting other secondary wake vorticity, although past theoretical studies have considered the influence of vorticity shed from the turbine hub (e.g. [7]). However, it is plausible that secondary vorticity plays an important role in development of wake instabilities, depending on its strength relative to the tip vortices. Fig. 1 shows a simplified illustration of the wake vorticity behind a turbine in a meridional section view. The red box contains the tip vortices in each returning wake segment, while the green box contains the tip vortex and the secondary spanwise vorticity of a single vortex sheet. We will now consider how each of these may affect the stability of the tip vortices.

Consider a turbine subjected to uniform steady axial inflow, with an additional small harmonic axial flow perturbation (caused by surface waves, for example). The harmonic variations in inflow will cause a corresponding variation in turbine loading, and therefore the strength of the shed tip vortex will also vary harmonically with the varying inflow. The effect of this is easiest to see when considering the meridional section view shown in Fig. 1, in which the tip vortices can be observed in a 2D framework. The following relation gives the strength of any individual tip vortex in the 2D framework, as a function of the inflow perturbation frequency ω (rad/s):

$$\Gamma_n = \Gamma_{steady} + \hat{\Gamma} sin(\Psi\theta + \Phi) \tag{1}$$

where $\hat{\Gamma}$ represents the harmonic amplitude of the shed tip vortex strength and θ is the circumferential position of the vortex. The parameters Ψ and Φ are given by:

$$\Psi = \frac{\omega}{\Omega N_B} \tag{2}$$

$$\Phi = 2\pi n \frac{\omega}{\Omega N_B} \tag{3}$$

where Ω represents the turbine rotational frequency in rad/s, N_B is the number of turbine blades and n is an integer that determines the streamwise location of the tip vortex.

If we consider the meridional view at $\theta = 0$ for simplicity, we can see that the relative strength of adjacent vortices will be governed by Φ, or more specifically, what we will call the "frequency ratio":

$$Frequency\ ratio = \frac{\omega}{\Omega N_B} \tag{4}$$

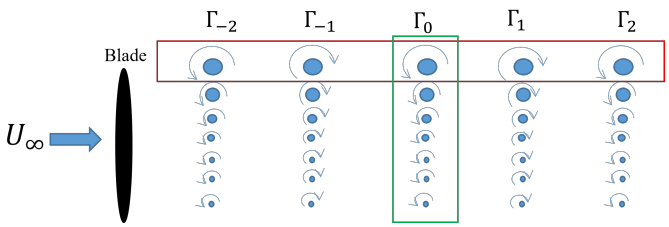

Fig. 1. Sketch of a meridional view of the vortex street behind a tidal turbine. The red box contains all tip vortices, the green box contains the tip vortex and the secondary spanwise vorticity of one vortex segment. The indicated directons of the vortices corresponds to frequency ratio $\omega/\Omega N_B = 0.5$.

Considering only the tip vortices (marked by the red box in Fig. 1), in the idealised case of all vortices being horizontally aligned, the stability of the vortex street depends on the frequency ratio. Past numerical studies, considering only the tip vortices, have found the ratio that produces the maximum growth rate of disturbances to be $\omega/\Omega N_B = 0.5$ [12], [13]. This corresponds to the tip vortices in the meridional view alternating between the maximum and minimum vortex strength. However, for a horizontally aligned (ideal) vortex street, an additional external perturbation would be required in order to trigger the instability. This external perturbation could be provided by the freestream turbulence.

Consider the tip vortex marked Γ_0 in Fig. 1. For a frequency ratio of 0.5, the induced velocity from adjacent tip vortices Γ_1 and Γ_{-1} cancel out, thus requiring an external perturbation in order to trigger instability. However, the induced velocity from the secondary wake vortices (marked in the green box in Fig. 1) will work to move the tip vortex Γ_0 towards Γ_{-1}, without any external perturbation necessary. The motion of tip vortices towards adjacent vortex segments leads to instability, resulting in leapfrogging. Depending on the strength of the secondary vortices relative to the spacing and strength of the tip vortices, it seems possible that the instability is triggered more quickly by secondary vorticity than by external perturbations such as the freestream turbulence. This is another reason why unsteady RANS simulations, where the dynamics of freestream turbulence is not captured as in LES, may still be useful to understand the mechanisms of turbine wake instability by focusing on the role of secondary vorticity.

C. Flow configuration

We simulate an axially oscillating uniform flow past a three-bladed horizontal-axis turbine, the geometry of which is based on a small-scale model turbine used in earlier experimental studies [21]. The rotor diameter, D, is 0.7 m and the rated tip-speed ratio (TSR) is 4. The blade design is based on that of an industrial tidal turbine, with a large blade thickness to prevent leading-edge flow separation. The chord Reynolds number at the mid-span of the blade is approximately 130,000 at the rated TSR (which we adopt throughout this study). Further details of the turbine design and performance can be found in [21].

Fig. 2 shows the computational domain employed. To reduce the computational cost, only one-third of a cylindrical domain containing a single blade is simulated with circumferentially periodic boundary conditions to account for the other two blades, although the use of such periodic conditions is known to suppress some of the instability modes that would be captured in a full cylindrical domain [13]. Slip wall conditions are applied to the centre and farfield domain boundaries, whereas outflow conditions (i.e., fixed condition for pressure and zero-gradient condition for velocities and turbulence quantities) are applied to the outlet boundary.

At the inlet boundary (located $2.35D$ upstream of the rotor plane) we apply a uniform but oscillatory streamwise velocity as a function of time, t, as

$$u = U_\infty \left[1 + a \sin(\omega t)\right] \tag{5}$$

where a and ω denote the amplitude and frequency (in rad/s) of velocity fluctuations, respectively, and $U_\infty = 1$ m/s is the mean flow speed. In this study we fix the amplitude at $a = 0.15$ (i.e., 15% of U_∞) whereas the frequency is varied to assess the effect of the frequency ratio, $\omega/N_B\Omega$ (where $N_B = 3$ is the number of blades and $\Omega = 11.43$ rad/s is the rotational frequency of each blade) on the stability of helical wake vortices. The freestream turbulence level is very low in this study.

D. Numerical methods

OpenFOAM employs an unstructured finite-volume method, but in this study we created a multi-block structured mesh for the entire computational domain. The blade surface is discretised into 232 cells in the chordwise direction (110 on each of the pressure and suction surfaces and 12 on the rounded trailing edge) and 79 cells in the spanwise direction, as shown in Fig. 2b. To reduce the computational cost, the standard wall functions are used with a wall-normal resolution of $y^+ \approx 60$. The use of wall functions is justified as the flow over the blade is mostly attached in this study. Some preliminary 2-D and 3-D steady simulations (not shown here for brevity) were also conducted to check the sufficiency of mesh resolution in the chordwise and spanwise directions, respectively. The total mesh size is approximately 17 million cells. More information on the preliminary mesh resolution studies can be found in [22].

The unsteady simulations were carried out using the 'pimpleDyMFoam' solver in OpenFOAM with second-order spatial discretisation schemes. Each simulation was run first with a large time-step size (corresponding to about 2 degrees of blade rotation) until the wake reaches the outlet of the domain, and then with a smaller time-step size (corresponding to about 0.2 degrees of blade rotation) to gather unsteady flow data.

III. Results

In the following we present results from the unsteady RANS simulations in the form of contour plots of vorticity in the turbine wake. The effects of unsteady

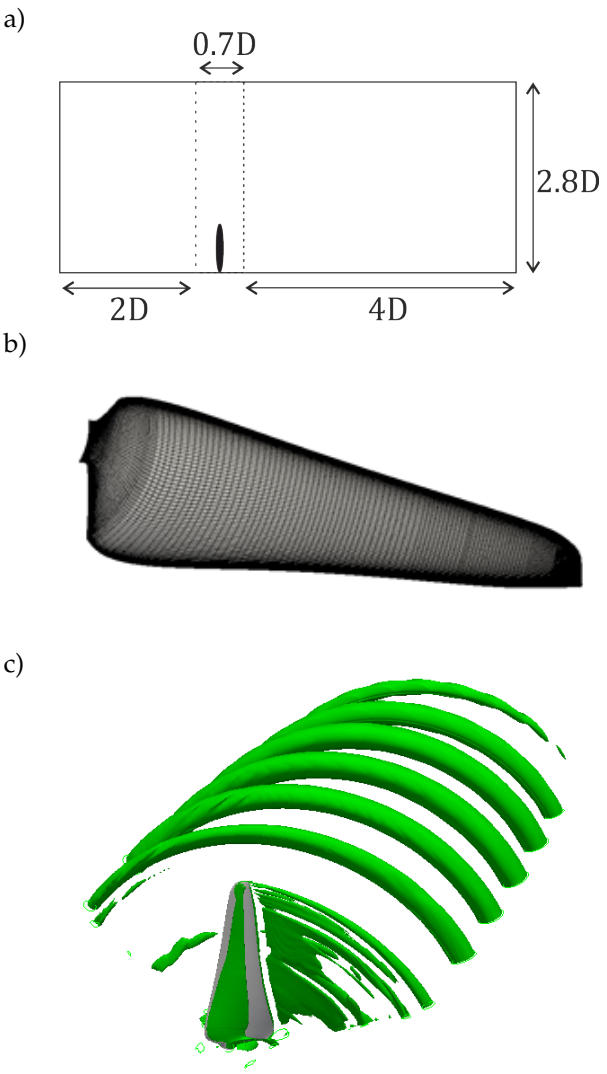

Fig. 2. a) Dimensions of the computational domain. b) Surface mesh of the turbine blade. c) Wake vorticity visualised using the Q criterion for steady flow, showing the periodic domain boundaries.

inflow on the loading and performance of the turbine are planned to be reported separately in the near future. Preliminary results can be found in [2].

Fig. 3 shows the unsteady turbine wakes for frequency ratios $\omega/\Omega N_B = 1/4,\ 1/2$ and $3/4$. For each frequency, meridional and radial views of the vorticity are shown, from the turbine plane to the exit plane. For all cases in Fig. 3 a regular pattern of wake development can be observed: initially the tip vortices are distinct and separate, but rapidly they become unstable and go through a transition period during which tip vortices group together and begin leapfrogging, after which a new regular vortex pattern emerges with a lower spatial frequency.

The number of tip vortices in each new grouping depends on the frequency ratio. This determines the spatial periodicity in wake vortex strength, and thus governs the relative motion of the tip vortices, as introduced in Section II-B. From Fig. 3, $\omega/\Omega N_B = 1/4$ and $3/4$ appear to lead to groups of 4 vortices, while $\omega/\Omega N_B = 1/2$ leads to groups of 2 vortices.The number of grouped vortices effectively determines the spatial frequency of the unsteady wake as it moves down-

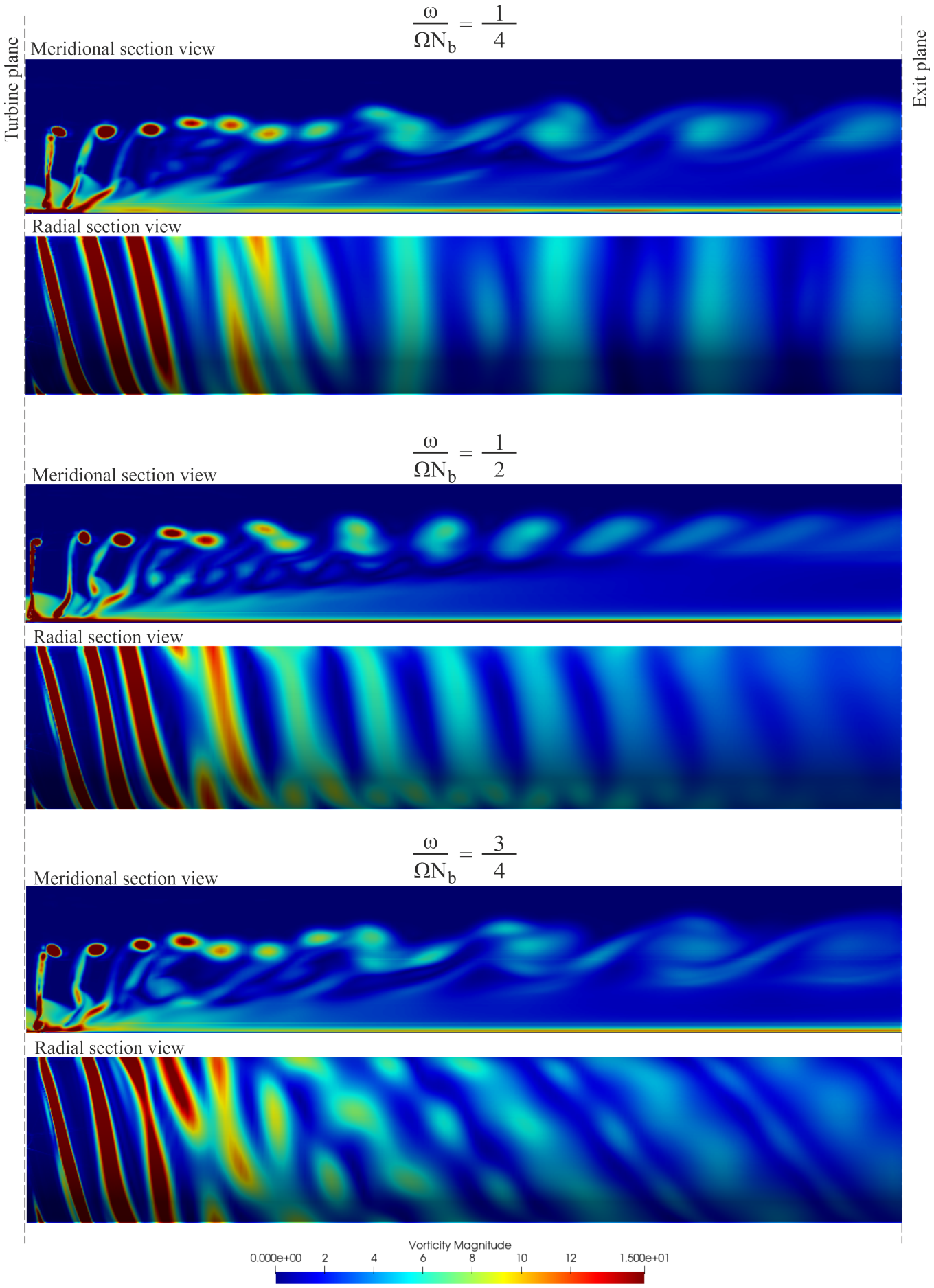

Fig. 3. Meridional and radial views of the wake vorticity behind the model tidal turbine, for three different frequency ratios. The visualisation is from the turbine plane to the exit plane.

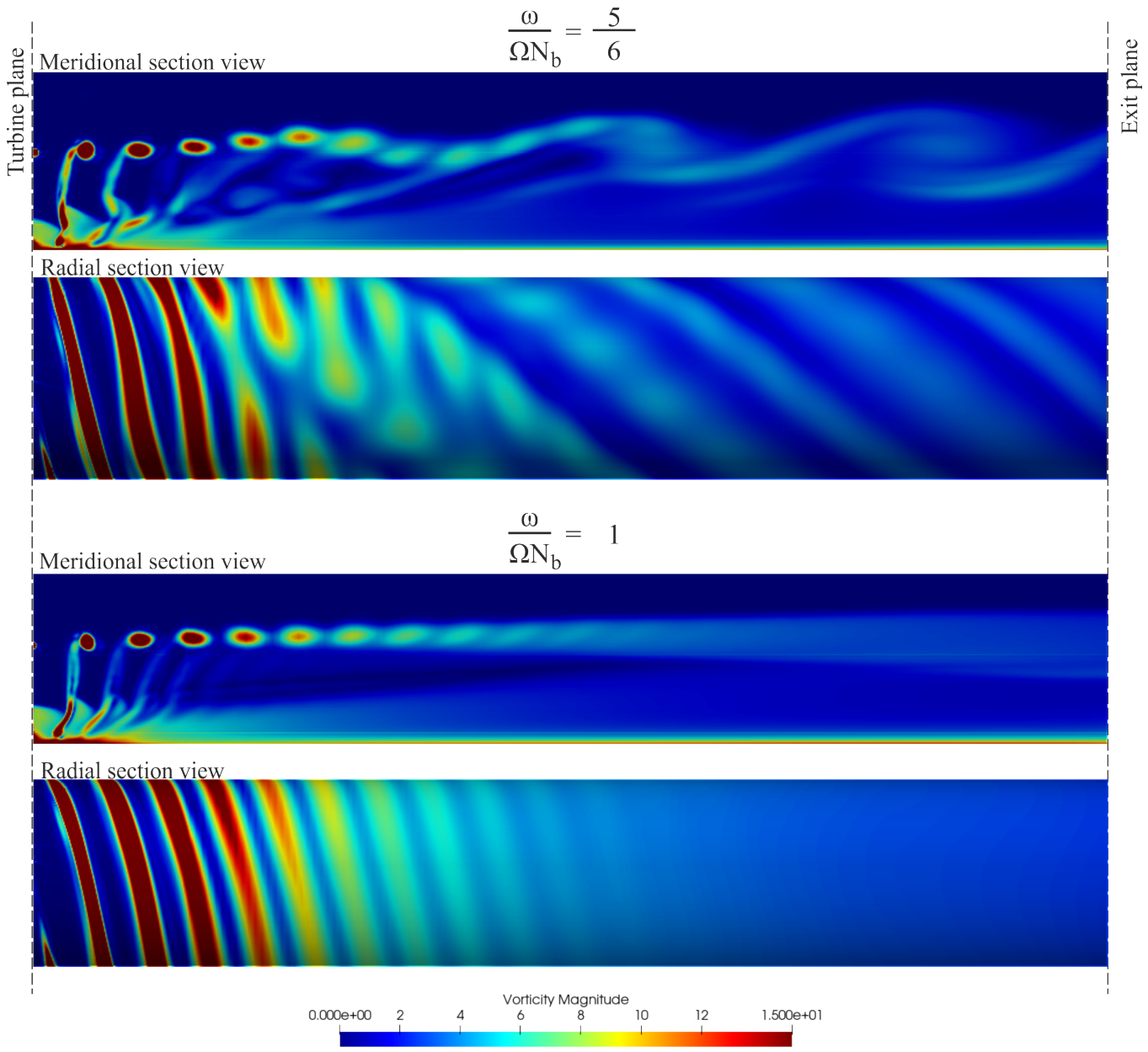

Fig. 4. Meridional and radial views of the wake vorticity behind the model tidal turbine, for two different frequency ratios. The visualisation is from the turbine plane to the exit plane.

stream.

The trend continues as the frequency ratio is increased. Fig. 4 shows the unsteady turbine wakes for frequency ratios $\omega/\Omega N_B = 5/6$ and 1. Once again the denominator in the frequency ratio appears to determine the number of vortices that gather to form new coherent groupings as the wake becomes unstable. For the case of $\omega/\Omega N_B = 5/6$ there appear to be approximately 6 vortices in each group. As the frequency ratio approaches 1 the spatial frequency of the downstream wake becomes longer and the interactions weaker. In the last case at the bottom of Fig. 4, for $\omega/\Omega N_B = 1$, the spatial frequency goes to zero and the wake is stable with no visible interactions between the tip vortices.

Not all frequency ratios produce regular patterns of grouped vortices in the unsteady wake. Fig. 5 shows a case at $\omega/\Omega N_B = 5/12$, which does not result in a clear wake periodicity in the downstream wake. Groups of 3 vortices, 2 vortices and single vortices can be observed. As such, the peridoicity of the wake as it moves downstream cannot be straightforwardly estimated.

If the frequency ratio is larger than 1 the wake should display the same trend of behaviours as for lower frequency ratios, according to the theory presented in Section II-B. As demonstrated above, the strength of adjacent tip vortices is determine by the phase relation $\Phi = 2\pi n\omega/\Omega N_B$ where n is an integer. This means that the wake behaviour is periodic in ω, such that the interactions in the range $\omega/\Omega N_B = 0-1$ are predicted to be the same in the range $\omega/\Omega N_B = 1-2$. However, at these high frequencies 3D annular effects begin to affect the wake dynamics more significantly. Fig. 6 shows

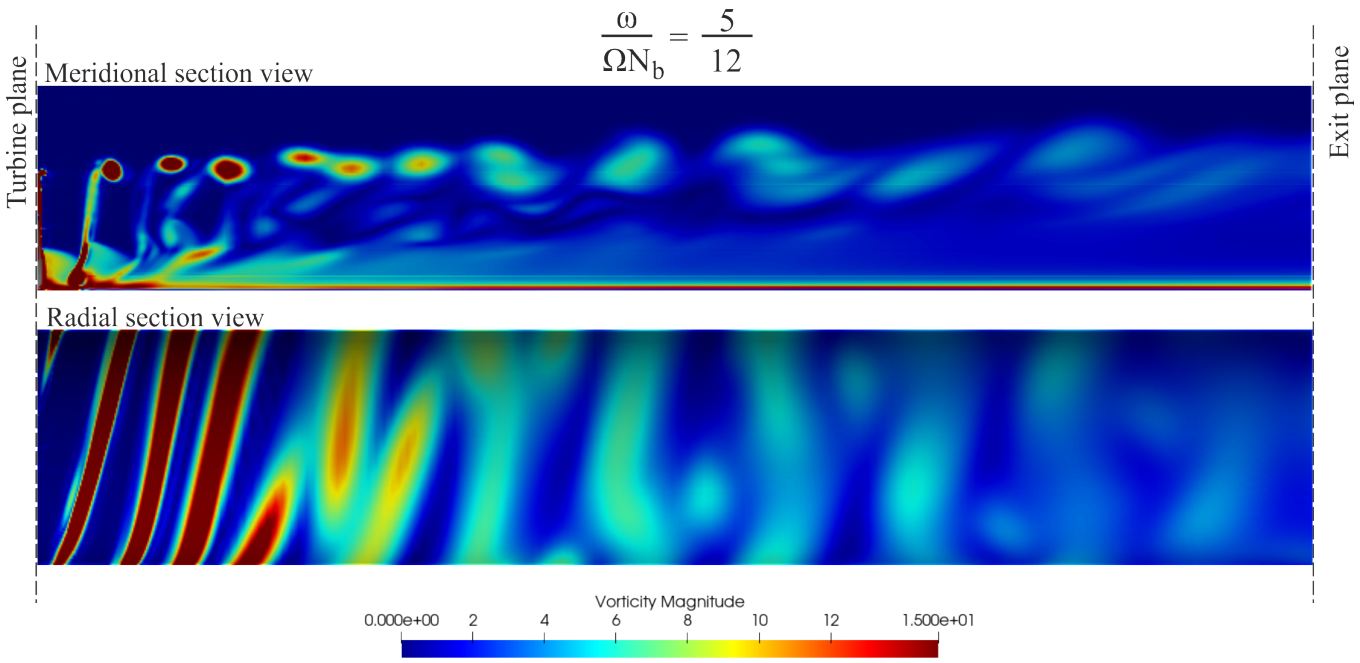

Fig. 5. Meridional and radial views of the wake vorticity behind the model tidal turbine, for frequency ratio $\omega/\Omega N_B = 5/12$. The visualisation is from the turbine plane to the exit plane.

the turbine wake for $\omega/\Omega N_B = 3/2$, which according to the theory should trigger the same type of wake interactions as that seen in Fig. 3 for $\omega/\Omega N_B = 1/2$. The meridional view in Fig. 6 does indeed suggest a grouping of 2 vortices as the wake becomes unstable. However the groupings are less clear and the interactions weaker. This is likely due to the significant wake fragmentation around the annulus, caused by the high frequency ratio. This can be seen in the radial view in Fig. 6: instead of the adjacent vortex segments interacting, as they did at the lower frequencies, the annular variation in vortex strength as seen in the radial view appears to dominate the wake dynamics.

IV. Discussion

The results presented in this paper highlight the importance of the frequency ratio of the unsteady inflow relative to the turbine rotation, ($\omega/\Omega N_B$), to the development of helical tip vortices behind a rotor. Of particular interest is that, when the frequency ratio is $1/m$ or $(m-1)/m$, where m is a positive integer, m neighbouring tip vortices appear to start leapfrogging and merging into a larger vortex. This results in a new large vortex street with a lower spatial frequency. For example, when $\omega/\Omega N_B = 1/2$, two neighbouring tip vortices appear to merge into a larger vortex, creating a new stable vortex street with a spacing twice as large as the original tip-vortex street. This is presumably because such a frequency ratio leads to a periodicity in the (initial) strength of m neighbouring tip vortices. When the frequency ratio is an integer m, the original tip-vortex street is stable as all tip vortices have the same initial strength.

When the frequency ratio is neither $1/m$, $(m-1)/m$ nor m, the helical wake tends to exhibit a strong instability leading to a complex deformation and merging of tip vortices. This suggests that the breakdown of tip vortices into turbulence may happen quicker in such cases, which may help shorten the near-wake length. However, as noted earlier, unsteady RANS simulations are unable to capture the exact process of tip vortex breakdown. To quantitatively assess the impact of the frequency ratio on the near-wake length, we would need a high-resolution LES study in the future.

Another important observation in this study is that, with the exception of cases where the frequency ratio is an integer, the tip vortices tend to start leapfrogging almost immediately after being shed from the blades. This early initiation of leapfrogging does not seem to be explained by the instability of tip vortices alone, because when the frequency ratio is $\omega/\Omega N_B = 0.5$, for example, the resulting tip vortex street (with stronger and weaker vortices arranged alternately) is supposed to be neutrally stable, meaning that it would require some additional disturbances in the flow to grow and trigger the leapfrogging motion (see Section II-B). However, this may be explained by the effects of "secondary" vortices (i.e., the vortices shed from the trailing edge of each blade section due to non-uniform blade loading across the span) inducing additional positive or negative streamwise velocities of tip vortices, changing the (otherwise equidistant) spacing of tip vortices.

V. Conclusions

This paper has presented an unsteady RANS study of the wake dynamics of a model tidal turbine undergoing oscillatory inflow conditions. The resulting tip vortex instabilities are explained with reference to the dynamics of a vortex street with varying vortex strengths, with secondary spanwise vorticity indicated

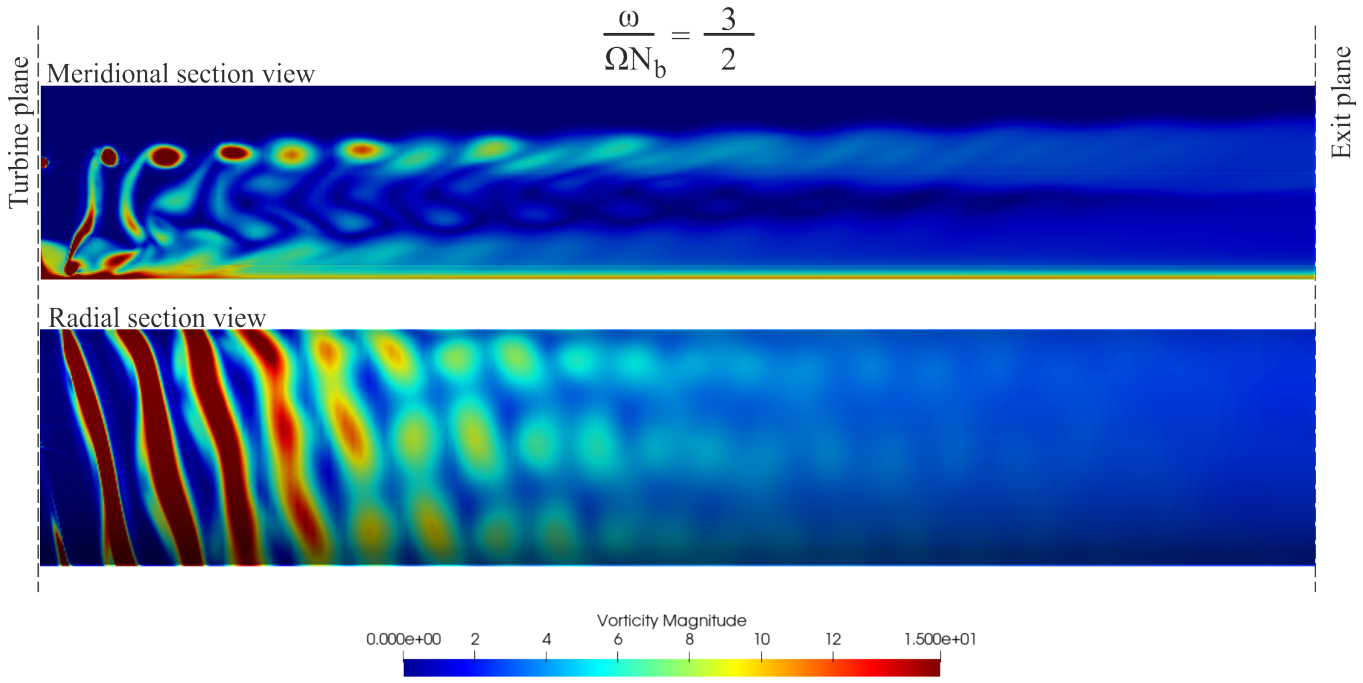

Fig. 6. Meridional and radial views of the wake vorticity behind the model tidal turbine, for frequency ratio $\omega/\Omega N_B = 3/2$. The visualisation is from the turbine plane to the exit plane.

as potentially playing a primary role in triggering the instabilities. When the frequency ratio $\omega/\Omega N_B$ could be expressed in the form of either $(m-1)/m$ or $1/m$, m being an integer, the wake instability was observed to cause tip vortices to congregate in groups of m vortices. At other frequencies the wake instability caused more irregular wake deformation and vortex merging. For $\omega/\Omega N_B = 1$ the wake was stable, and for higher frequencies 3D annular effects started to become more dominant. These results have implications for wake development and recovery in unsteady flow conditions caused by e.g. surface waves or turbine motion, and therefore for the streamwise spacing of turbines in arrays.

REFERENCES

[1] C. L. Sequeira and R. J. Miller, "Unsteady gust response of tidal stream turbines," *Proc. IEEE/MTS OCEANS*, 2014.

[2] A. S. M. Smyth and A. M. Young, "Three-dimensional unsteady hydrodynamic modelling of tidal turbines," *Proc. 13th European Wave and Tidal Energy Conference (EWTEC)*, 2019.

[3] L. E. M. Lignarolo, D. Ragni, F. Scarano, C. J. Simão Ferreira, and G. J. W. van Bussel, "Tip-vortex instability and turbulent mixing in wind-turbine wakes," *Journal of Fluid Mechanics*, vol. 781, pp. 467–493, 2015.

[4] S. E. Widnall, "The stability of a helical vortex filament," *Journal of Fluid Mechanics*, vol. 54, pp. 641–663, 1972.

[5] B. P. Gupta and R. G. Loewy, "Theoretical analysis of the aerodynamic stability of multiple, interdigitated helical vortices," *AIAA Journal*, vol. 12, pp. 1381–1387, 1974.

[6] Y. Fukumoto and T. Miyazaki, "Three-dimensional distortions of a vortex filament with axial velocity," *Journal of Fluid Mechanics*, vol. 222, pp. 369–416, 1991.

[7] V. L. Okulov and J. N. Sørensen, "Stability of helical tip vortices in a rotor far wake," *Journal of Fluid Mechanics*, vol. 576, pp. 1–25, 2007.

[8] M. Felli, R. Camussi, and F. Di Felice, "Mechanisms of evolution of the propeller wake in the transition and far fields," *Journal of Fluid Mechanics*, vol. 682, pp. 5–53, 2011.

[9] H. U. Quaranta, H. Bolnot, and T. Leweke, "Long-wave instability of a helical vortex," *Journal of Fluid Mechanics*, vol. 780, pp. 687–716, 2015.

[10] H. U. Quaranta, M. Brynjell-Rahkola, T. Leweke, and D. S. Henningson, "Local and global pairing instabilities of two interlaced helical vortices," *Journal of Fluid Mechanics*, vol. 863, pp. 927–955, 2019.

[11] J. N. Sørensen and W. Z. Shen, "Numerical modeling of wind turbine wakes," *Journal of Fluids Engineering*, vol. 124, pp. 393–399, 2002.

[12] S. Ivanell, R. Mikkelsen, J. N. Sørensen, and D. Henningson, "Stability analysis of the tip vortices of a wind turbine," *Wind Energy*, vol. 13, pp. 705–715, 2010.

[13] S. Sarmast, R. Dadfar, R. F. Mikkelsen, P. Schlatter, S. Ivanell, J. N. Sørensen, and D. S. Henningson, "Mutual inductance instability of the tip vortices behind a wind turbine," *Journal of Fluid Mechanics*, vol. 755, pp. 705–731, 2017.

[14] J. N. Sørensen, R. Mikkelsen, S. Sarmast, S. Ivanell, and D. Henningson, "Determination of wind turbine near-wake length based on stability analysis," *Journal of Physics: Conference Series*, vol. 524, p. 012155, 2014.

[15] T. Nishino and R. H. J. Willden, "Low-order modelling of blade-induced turbulence for RANS actuator disk computations of wind and tidal turbines," in *Wind Energy - Impact of Turbulence*. Springer, 2014, pp. 153–158.

[16] I. Neunaber, M. Hölling, and M. Obligado, "Leading effect for wind turbine wake models," *SSRN*, March 2023. http://dx.doi.org/10.2139/ssrn.4371893.

[17] D. Marten, C. O. Paschereit, X. Huang, M. Meinke, W. Schröder, J. Müller, and K. Oberleithner, "Predicting wind turbine wake breakdown using a free vortex wake code," *AIAA Journal*, vol. 58, 2020.

[18] K. Brown, D. Houck, D. Maniaci, C. Westergaard, and C. Kelley, "Accelerated wind-turbine wake recovery through actuation of the tip-vortex instability," *AIAA Journal*, vol. 60, 2022.

[19] C. J. Greenshields, "OpenFOAM User Guide, version 6," 2018.

[20] F. R. Menter, "Two-equation eddy-viscosity turbulence models for engineering applications," *AIAA Journal*, vol. 32, pp. 1598–1605, 1994.

[21] A. M. Young, J. R. Farman, and R. J. Miller, "Load alleviation technology for extending life in tidal turbines," *Proc. 2nd International Conference on Renewable Energies Offshore (RENEW)*, 2016.

[22] A. S. M. Smyth, "Three-dimensional unsteady hydrodynamics of tidal turbines (PhD Thesis)," *Cambridge University*, 2019.